02-09

February 2009

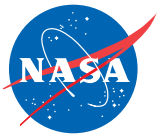

TECH BRIEFS

NATIONAL AERONAUTICS AND SPACE ADMINISTRATION

INTRODUCTION

Tech Briefs are short announcements of innovations originating from research and development activities of the National Aeronautics and Space Administration. They emphasize information considered likely to be transferable across industrial, regional, or disciplinary lines and are issued to encourage commercial application.

Availability of NASA Tech Briefs and TSPs

Requests for individual Tech Briefs or for Technical Support Packages (TSPs) announced herein should be addressed to

National Technology Transfer Center

Telephone No. **(800) 678-6882** or via World Wide Web at **http://www.nttc.edu/about/contactus.asp**

Please reference the control numbers appearing at the end of each Tech Brief. Information on NASA's Innovative Partnerships Program (IPP), its documents, and services is also available at the same facility or on the World Wide Web at **http://ipp.nasa.gov**.

Innovative Partnerships Offices are located at NASA field centers to provide technology-transfer access to industrial users. Inquiries can be made by contacting NASA field centers listed below.

NASA Field Centers and Program Offices

Ames Research Center
Lisa L. Lockyer
(650) 604-1754
lisa.l.lockyer@nasa.gov

Dryden Flight Research Center
Gregory Poteat
(661) 276-3872
greg.poteat@dfrc.nasa.gov

Glenn Research Center
Kathy Needham
(216) 433-2802
kathleen.k.needham@nasa.gov

Goddard Space Flight Center
Nona Cheeks
(301) 286-5810
nona.k.cheeks@nasa.gov

Jet Propulsion Laboratory
Ken Wolfenbarger
(818) 354-3821
james.k.wolfenbarger@jpl.nasa.gov

Johnson Space Center
Michele Brekke
(281) 483-4614
michele.a.brekke@nasa.gov

Kennedy Space Center
David R. Makufka
(321) 867-6227
david.r.makufka@nasa.gov

Langley Research Center
Martin Waszak
(757) 864-4015
martin.r.waszak@nasa.gov

Marshall Space Flight Center
Jim Dowdy
(256) 544-7604
jim.dowdy@msfc.nasa.gov

Stennis Space Center
John Bailey
(228) 688-1660
john.w.bailey@nasa.gov

Carl Ray, Program Executive
Small Business Innovation Research (SBIR) & Small Business Technology Transfer (STTR) Programs
(202) 358-4652
carl.g.ray@nasa.gov

Doug Comstock, Director
Innovative Partnerships Program Office
(202) 358-2560
doug.comstock@nasa.gov

02-09 February 2009

TECH BRIEFS

NATIONAL AERONAUTICS AND SPACE ADMINISTRATION

Measuring Low Concentrations of Liquid Water in Soil

Electrical-impedance measurements serve as sensitive indications of moisture content.

NASA's Jet Propulsion Laboratory, Pasadena, California

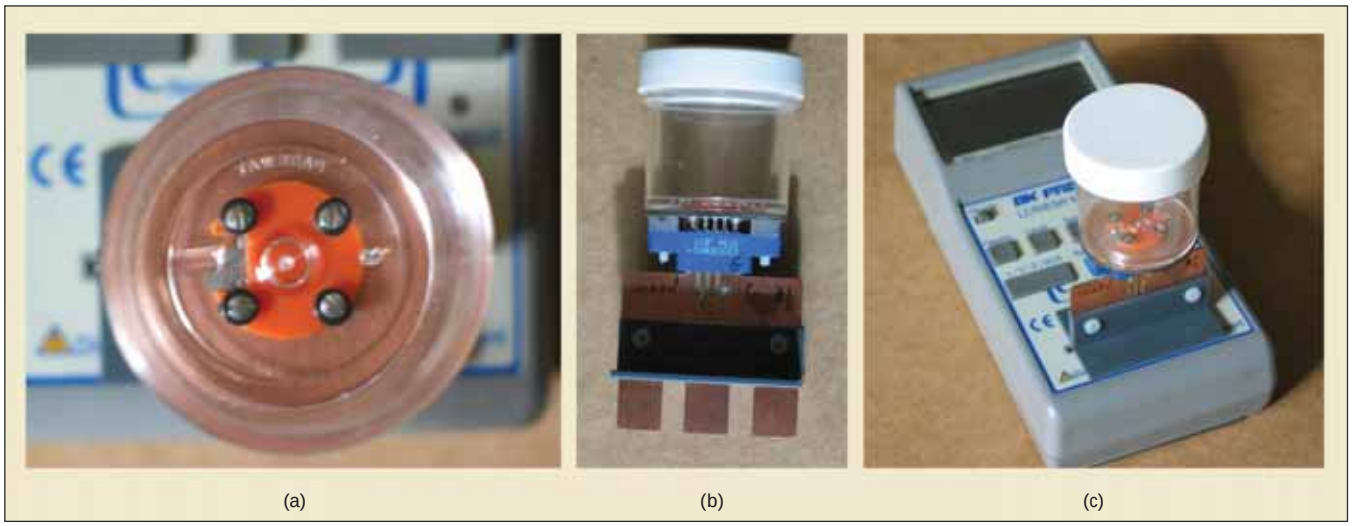

Figure 1. A **Sample Chamber Containing a Four-Electrode Probe** is mounted on a printed-circuit board that is plugged into a commercial impedance spectrometer: (a) top view of the soil moisture cup showing the four probes that are spaced 11.18 mm apart; (b) side view of soil moisture chamber inserted into printed wiring board that inserts into the LCR meter, and (c) LCR meter with soil-measuring cup.

An apparatus has been developed for measuring the low concentrations of liquid water and ice in relatively dry soil samples. Designed as a prototype of instruments for measuring the liquid-water and ice contents of Lunar and Martian soils, the apparatus could also be applied similarly to terrestrial desert soils and sands. The high sensitivity of this apparatus is best appreciated via a comparison: Whereas soil moisture contents of agricultural interest range between 3 and 30 weight percent, this apparatus is capable of measuring moisture contents from 0.01 to 10 weight percent (at room temperature). Moreover, it has been estimated that optimization of the design of the apparatus could enable measurement of moisture contents as low as 1 part per million by weight.

The apparatus is a special-purpose impedance spectrometer: Its design is based on the fact that the electrical behavior of a typical soil sample is well approximated by a network of resistors and capacitors in which resistances decrease and capacitances increase (and, hence, the magnitude of impedance decreases) with increasing water content. The apparatus includes a commercial impedance

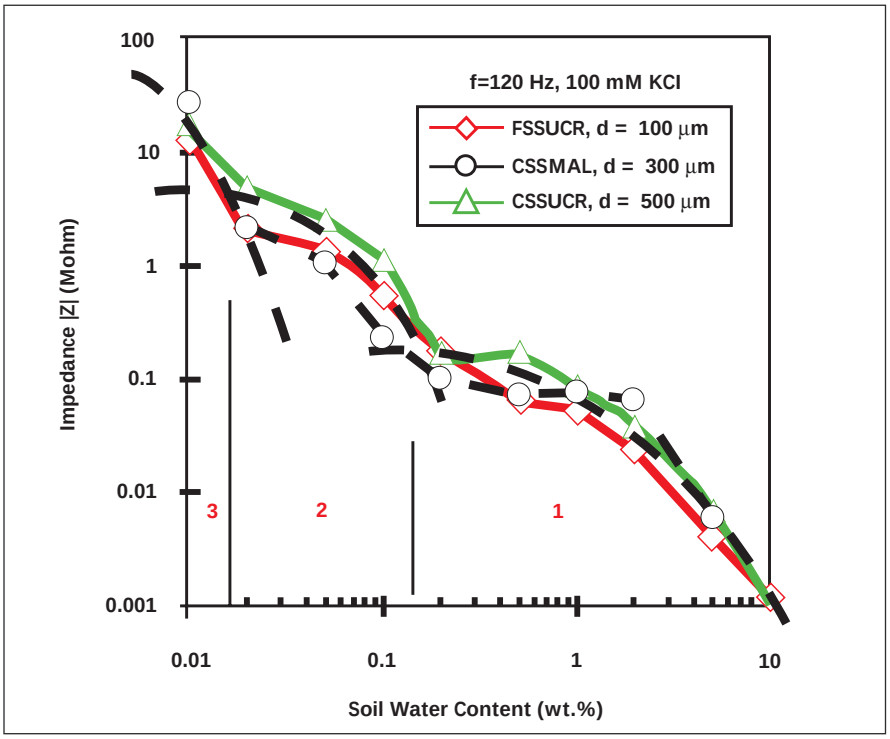

Figure 2. **Three Regions** measured by the impedance spectrometer that are explained by the soil moisture model. Measurements were obtained from fine silica sand and two samples of coarse silica sand with a diameter "d". The soil water was doped with 100 mM KCl and measured at a frequency of 100 Hz. (Note: FSSUCR is fine silica sand from the University of California, Riverside; CSSMAL is coarse silica sand from Mallinckrodt Chemicals; and CSSUCR is coarse silica sand from the University of California, Riverside.)

spectrometer and a custom sample chamber. Four stainless-steel screws at the bottom of the jar are used as electrodes of a four-point impedance probe. The leads from the electrodes are routed to a 10-pin connector that is plugged into a printed-circuit board that, in turn, is plugged into the impedance spectrometer (see Figure 1). Special precautions were taken in constructing the printed-circuit board to shield the signal conductors to enable measurement of impedances as high as 3 GΩ, thereby enabling measurement of very low levels of moisture. The lower limit of impedance measurable by this apparatus is 100 Ω.

For a typical measurement run, a sample of soil is placed in the jar and the magnitude and phase angle of impedance are measured at fixed frequencies of 100 Hz, 120 Hz, 1 kHz, 10 kHz, and 100 kHz, using applied AC potentials of 50 mV, 250 mV, and 1 V. The measurement data can then be plotted and analyzed to estimate water content, as illustrated by the example of Figure 2.

This work was done by Martin Buehler of Caltech for NASA's Jet Propulsion Laboratory. Further information is contained in a TSP (see page 1).

In accordance with Public Law 96-517, the contractor has elected to retain title to this invention. Inquiries concerning rights for its commercial use should be addressed to:

Innovative Technology Assets Management
JPL
Mail Stop 202-233
4800 Oak Grove Drive
Pasadena, CA 91109-8099
E-mail: iaoffice@jpl.nasa.gov

Refer to NPO-41822, volume and number of this NASA Tech Briefs *issue, and the page number.*

The Mars Science Laboratory Touchdown Test Facility

NASA's Jet Propulsion Laboratory, Pasadena, California

In the Touchdown Test Program for the Mars Science Laboratory (MSL) mission, a facility was developed to use a full-scale rover vehicle and an overhead winch system to replicate the Skycrane landing event. A driving requirement for the testing facility was the need to support a load of 5,000 lb (2,268 kg) at a minimum height of 13 m. Few facilities at JPL qualify with enough height, leaving the Building 280 Static Test Tower as the logical choice. However, this facility is popular, so an additional requirement was that the MSL test facility be temporary, and be able to be disassembled in a matter of a week or two, be stored for a period of time, and then be reassembled again quickly for V&V (verification and validation) testing.

The Building 280 Test Tower is a 50-ft-tall (15-m) steel tower structure measuring approximately 15 by 15 ft (4 by 4 m). Overhead pulleys were mounted on a new cantilevered frame so that testing could be conducted on the south face of the tower. Landing surfaces consisted of flat and sloped granular media, and rigid, planar surfaces. Various combinations of rocks and slopes were studied. Information gathered in these tests was vital for validating the rover analytical model, validating design and system behavior assumptions, and for exploring events and phenomena that are either very difficult or too costly to model in a credible way.

This work was done by Christopher White; John Frankovich; Phillip Yates; George H. Wells, Jr.; and Robert Losey of Caltech for NASA's Jet Propulsion Laboratory. NPO-45847

Non-Contact Measurement of Density and Thickness Variation in Dielectric Materials

An improved nondestructive inspection method uses terahertz energy for density and thickness mapping in dielectric, ceramic, and composite materials.

John H. Glenn Research Center, Cleveland, Ohio

This non-contact, single-sided terahertz electromagnetic measurement and imaging method characterizes microstructural (e.g., spatially-lateral density) and thickness variation in dielectric (insulating) materials. This method was demonstrated for space shuttle external tank sprayed-on foam insulation and has been designed for use as an inspection method for current and future NASA thermal protection systems and other dielectric material inspection applications where no contact can be made with the sample due to fragility and it is impractical to use ultrasonic methods (the latter methods require the sample under test to be immersed in liquid).

To provide some background, a basic pulse-echo terahertz thickness measurement for a dielectric (insulating) material is made by sending terahertz energy via a transceiver into and through the material backed by a metallic (electrically conducting) plate that reflects the terahertz energy back to the transceiver. The terahertz transceiver is separated from the dielectric sample by an air path. Thickness values are calculated using the time delay between the first front surface (*FS*) and the first substrate/reflector plate echo (*BS*) and knowledge of velocity according to distance = velocity × time delay. In a similar fashion, the velocity through the material can be determined by knowing thickness. Velocity is an important parameter because density can be derived from velocity using established velocity-density relationships for the dielectric material.

The new method allows characterization of thickness without prior knowledge of velocity and characterization of velocity without prior knowledge of thickness, and it does so using the same set of measurements. The method is still based on pulse-echo measurements,

and uses echoes off of the reflector plate with (*BS*) and without the sample present (*M*"), as well as using the echo off of the sample front surface (*FS*). (The FS echo may require specialized signal processing to "de-noise" and amplify it if it is received off of a foam front surface.)

This work was done by Ron Roth for Glenn Research Center. Further information is contained in a TSP (see page 1).

Inquiries concerning rights for the commercial use of this invention should be addressed to NASA Glenn Research Center, Innovative Partnerships Office, Attn: Steve Fedor, Mail Stop 4–8, 21000 Brookpark Road, Cleveland, Ohio 44135. Refer to LEW-18262-1/3-1.

Compact Microwave Fourier Spectrum Analyzer

Large delays needed for time-domain autocorrelations would be realized photonically.

NASA's Jet Propulsion Laboratory, Pasadena, California

A compact photonic microwave Fourier spectrum analyzer [a Fourier-transform microwave spectrometer, (FTMWS)] with no moving parts has been proposed for use in remote sensing of weak, natural microwave emissions from the surfaces and atmospheres of planets to enable remote analysis and determination of chemical composition and abundances of critical molecular constituents in space.

The instrument is based on a Bessel beam (light modes with non-zero angular momenta) fiber-optic elements (see figure). It features low power consumption, low mass, and high resolution, without a need for any cryogenics, beyond what is achievable by the current state-of-the-art in space instruments. The instrument can also be used in a wide-band scatterometer mode in active radar systems.

The basic advantage of the proposed instrument is its wide bandwidth along with high resolution, enabling microwave hyperimaging of the planetary atmospheres and surfaces. For example, the analyzer will have similar resolution to the Cassini Titan Radar Mapper operating in the scatterometer mode, and will have at least two orders of magnitude wider bandwidth, compared with the same instrument operating in the radiometer mode. This will allow collecting a hundred times more data during the same observation period.

The analyzer has significant advantages for remote detection of chemical components from space. It uses microwave radiation to record the rotational spectrum of a molecule in the microwave spectral region, i.e., between approximately 6 GHz and 40 GHz. For instance, FTMWS can be used for the accurate remote detection of water vapor as well as for the study of hydrogen isotopic ratio.

The analyzer has a very long, mile-range, maximum delay realized with photonics techniques. This capability is ultimately crucial for achieving a high resolution with the Fourier transform spectrum analyzer. To obtain the 1-MHz spectral resolution necessary for resolving the microwave emission spectrum of water in remote sensing, it would ordinarily be necessary to use microwave delay lines having lengths up to 300 m. Such long microwave delay lines would not be practical. However, the instrument would exploit the fact that compact delay lines can be realized photonically.

It has Fellgett (multiplex) advantage taken from Fourier spectroscopy. A typical microwave spectrum analyzer sequentially measures the microwave power within each of a number of narrow spectral bands. The new instrument would simultaneously measure the time-domain autocorrelations of the microwave emission signal of interest using a number of different delays, then calculate the spectrum of that signal by use of a fast Fourier transform. Hence, the instrument would constantly and simultaneously provide data on all the bands of the spectrum.

It has all the advantages of a static Fourier transform spectrometer. There are no moving parts, which eliminates many potential mechanical problems onboard the spacecraft. The instrument has no need for a reference laser since the detector array samples the interferogram always at the same points. The analyzer obtains full interferogram at once so it is insensitive to the flicker noise or fluctuations of the input signal. This is critical, e.g., for spectroscopy of a constantly changing planetary environment.

As shown in the figure, the incoming

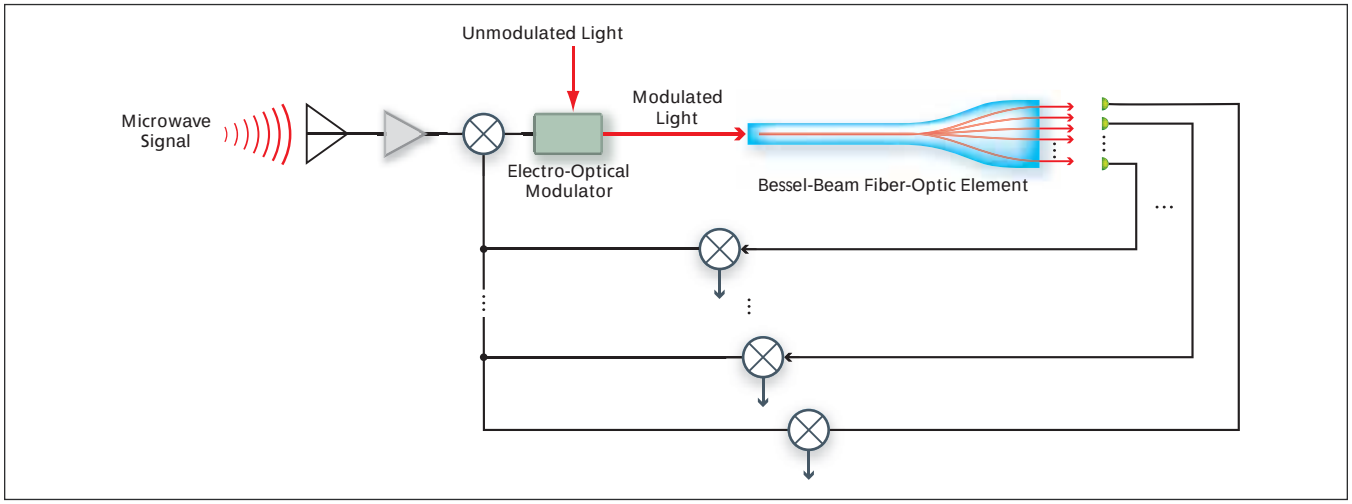

The **Microwave Spectrum Would Be Translated** to the optical spectrum, wherein compact delay lines can be realized by use of highly dispersive optical elements.

microwave signal would be amplified and applied to the input terminal of an electro-optical modulator, which would impress the microwave signal as modulation onto a beam of light. The light would enter a Bessel-beam fiber-optic element, which is essentially an optical waveguide that tapers to a wider aperture at its output end. A Bessel-beam fiber-optic element acts as a highly dispersive radiator horn, roughly equivalent to a bundle of optical fibers of different lengths. The dispersion in a Bessel-beam fiber-optic element is so great as to afford delays ranging from about 10 ps to about 1 μs. In this instrument, the light arriving at each location on the output plane of the dispersive optical element would have a different delay, and so an array of photodiodes would be placed on that output plane to sample signals at various increments of delay. The variously delayed microwave outputs of the photodiodes would be used to obtain the required autocorrelation data.

This work was done by Anatoliy Savchenkov, Andrey Matsko, Dmitry Strekalov, and Lute Maleki of Caltech for NASA's Jet Propulsion Laboratory. Further information is contained in a TSP (see page 1).

In accordance with Public Law 96-517, the contractor has elected to retain title to this invention. Inquiries concerning rights for its commercial use should be addressed to:

Innovative Technology Assets Management
JPL
Mail Stop 202-233
4800 Oak Grove Drive
Pasadena, CA 91109-8099
(818) 354-2240
E-mail: iaoffice@jpl.nasa.gov

Refer to NPO-43992, volume and number of this NASA Tech Briefs *issue, and the page number.*

InP Heterojunction Bipolar Transistor Amplifiers to 255 GHz

These amplifiers can be used in millimeter-wave imaging systems for weapons detection and airport security, and for radar instruments.

NASA's Jet Propulsion Laboratory, Pasadena, California

Two single-stage InP heterojunction bipolar transistor (HBT) amplifiers operate at 184 and 255 GHz, using Northrop Grumman Corporation's InP HBT MMIC (monolithic microwave integrated circuit) technology. At the time of this reporting, these are reported to be the highest HBT amplifiers ever created. The purpose of the amplifier design is to evaluate the technology capability for high-frequency designs and verify the model for future development work.

MMIC amplifier operating frequencies have pushed past 200 GHz and into submillimeter wave frequencies. The main driver has been in demand for millimeter-wave radiometers and high-resolution, all-weather imaging systems.

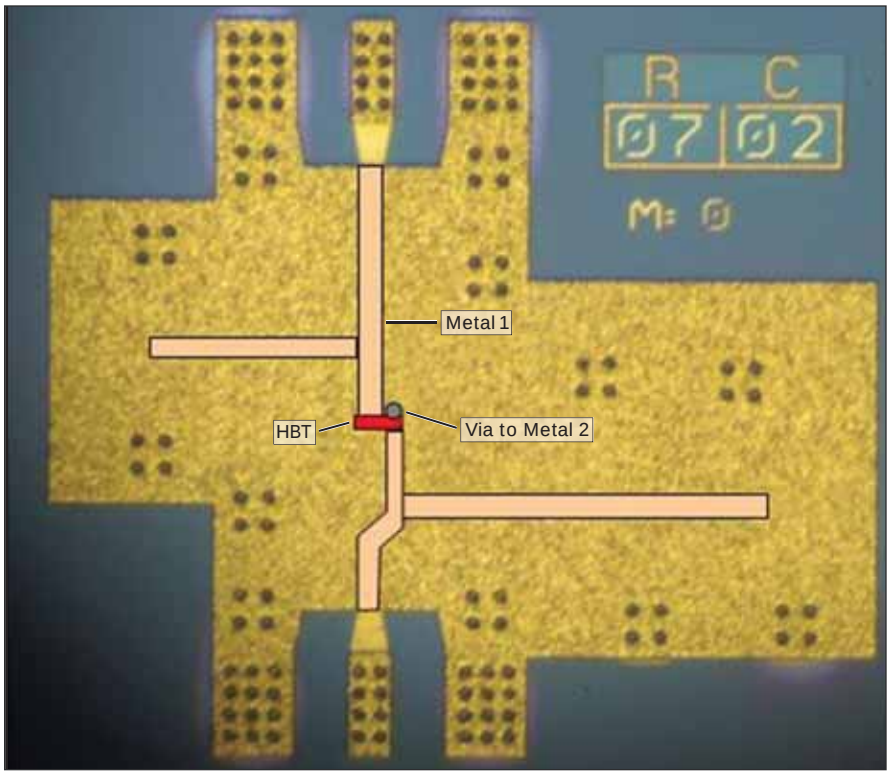

A microphotograph shows the **255-GHz Amplifier MMIC**. A second metal serves as a ground plane and covers most of the circuit area. The transmission lines and HBT device are "drawn" in the photograph. Die size is 0.55 mm × 0.55 mm.

MMIC power amplifiers have a variety of applications for ground-based and future space-based telescopes for astrophysics, as well as in local oscillators for heterodyne receivers in Earth and planetary science instruments. They can be used in millimeter-wave imaging systems to provide sensitive hidden-weapons detections, airport security imaging systems, or other homeland security portable imaging sensors. Power amplifiers can also be used in transmitters for radar instruments and commercial laboratory power sources.

While HEMT amplifiers are traditionally used for low noise receivers due to their low noise properties, HBT amplifiers can be used as power sources due to the nature of their material properties, traditionally higher breakdown voltages and potentially higher efficiency.

A demonstration of the MMIC HBT amplifier showed results approaching the sub-millimeter-wave regime (~300 GHz) and showed the highest reported gain of 3.5 dB for a single-stage HBT amplifier at 255 GHz. The common emitter topology was chosen due to its stability at high frequencies. Distributed transmission lines and matching components were realized using an inverted microstrip configuration, and were implemented in a two-metal process with BCB (benzocyclobutene) dielectric. The primary advantage of this configuration is low inductance to ground compared with traditional microstrip designs.

This work was done by Vesna Radisic, Donald Sawdai, Dennis Scott, William Deal, Linh Dang, Danny Li, Abdullah Cavus, Richard To, and Richard Lai of Northrop Grumman Corporation, and Lorene Samoska, King Man Fung, and Todd Gaier of Caltech for NASA's Jet Propulsion Laboratory. The contributors would like to acknowledge the support of Dr. Mark Rosker and the Army Research Laboratory. This work was supported by the DARPA SWIFT Program and Army Research Laboratory under the DARPA MIPR no.06-U037 and ARL Contract no. W911QX-06-C-0050. NPO-45465

Combinatorial Generation of Test Suites

NASA's Jet Propulsion Laboratory, Pasadena, California

Testgen is a computer program that generates suites of input and configuration vectors for testing other software or software/hardware systems. As systems become ever more complex, often, there is not enough time to test systems against all possible combinations of inputs and configurations, so test engineers need to be selective in formulating test plans. Testgen helps to satisfy this need: In response to a test-suite-requirement-specification model, it generates a minimal set of test vectors that satisfies all the requirements.

Testgen generates test cases following a combinatorial approach, but instead of generating all possible combinations across all test factors, it generates a test suite covering all possible combinations among user-specified groups of test factors. Testgen affords three main benefits:

- The level of coverage of the test space can be increased or decreased easily by modifying the test model. Hence, the rigor of testing can be adjusted according to availability of time and resources.
- Within a test model, degrees of combinations can be adjusted separately for different subsystems.
- Typically, Testgen generates test cases in seconds, whereas manual generation of the same test cases takes hours, and Testgen never omits desired combinations or includes redundant test cases.

This program was written by Anthony C. Barrett and Daniel L. Dvorak of Caltech for NASA's Jet Propulsion Laboratory. Further information is contained in a TSP (see page 1).

This software is available for commercial licensing. Please contact Karina Edmonds of the California Institute of Technology at (626) 395-2322. Refer to NPO-45921.

In-Phase Power-Combined Frequency Tripler at 300 GHz

This compact, tunable, broadband, high-power design is suitable for radar as well as for driving imaging arrays of heterodyne spectrometers.

NASA's Jet Propulsion Laboratory, Pasadena, California

This design starts with commercial 85- to 115-GHz sources that are amplified to as much as 250 mW using power amplifiers developed for the Herschel Space Observatory. The frequency is then tripled using a novel waveguide GaAs Schottky diode frequency tripler. This planar diode produces 26 mW at 318 GHz. Peak conversion efficiency is over 15 percent, and the measured bandwidth of about 265–330 GHz is limited more by the driving source than by the tripler itself.

This innovation is based on an integrated circuit designed originally for a single-chip 260- to 340-GHz balanced tripler. The power-combined version has two mirror-image tripler chips that are power-combined in-phase in a single waveguide block using a compact Y-junction divider at the input waveguide, and a Y-junction combiner at the output waveguide. The tripler uses a split-block waveguide design with two independent DC bias lines. The input waveguide is split in two by a Y-junction to evenly feed two circuits, each featuring six Schottky planar varactor diodes of about 16 fF on a 5 μm-thick GaAs membrane. The chips are mounted in two independent channels that run between their respective input and output waveguides. The two reduced-height output waveguides are combined by a Y-junction that is seen by each branch of the circuit as a simple waveguide step.

On each chip, an E-plane probe located in the input waveguide couples the signal at the input frequency to a suspended microstrip line. This line has several sections of low and high impedance that are used to match the diodes at the input and output frequencies, and to prevent the third harmonic from leaking into the input waveguide. The third harmonic produced by the diodes is coupled to the output waveguide by a second E-plane probe. In order to balance the circuit, the dimensions of both the channel and the circuit are chosen to cut off the TE-mode at the second (idler) frequency. The dimensions of the output waveguide ensure that the second harmonic is cut off at all frequencies measured, and the balanced geometry of the chips ensures that the power at the fourth harmonic of the input is strongly suppressed.

The tripler can be used to pump subharmonic mixers used as high-resolution spectrometers to measure temperature, pressure, velocity, and chemical composition of planetary atmospheres. The high output power makes this source ideal for driving frequency multipliers to very high frequencies. For example, the Earth observing system microwave limb sounder (EOS-MLS) instrument has a 2.5-THz channel. High power also makes this source suitable for radars as well as for driving imaging arrays of heterodyne spectrometers.

This work was done by Alain Maestrini of the Université Pierre et Marie Curie and John Ward, Robert Lin, John Gill, Choonsup Lee, Imran Mehdi, Hamid Javadi, and Goutam Chattopadhyay of Caltech for NASA's Jet Propulsion Laboratory.

In accordance with Public Law 96-517, the contractor has elected to retain title to this invention. Inquiries concerning rights for its commercial use should be addressed to:

Innovative Technology Assets Management JPL, Mail Stop 202-233, 4800 Oak Grove Drive, Pasadena, CA 91109-8099, E-mail: iaoffice@jpl.nasa.gov, Refer to NPO-45479, volume and number of this NASA Tech Briefs *issue, and the page number.*

Electronic System for Preventing Airport Runway Incursions

Portable units would perform monitoring, signaling, and automatic warning functions.

Marshall Space Flight Center, Alabama

The figure is a block diagram of a proposed system of portable illuminated signs, electronic monitoring equipment, and radio-communication equipment for preventing (or taking corrective action in response to) improper entry of aircraft, pedestrians, or ground vehicles onto active airport runways. Such an entry, denoted a runway incursion, poses a risk of collision with an aircraft properly moving on the affected runway. The major causes of runway incursions are mistakes by pilots, ground-vehicle drivers, and control-tower personnel. Heretofore, there have been no automated, systematic, reliable means of monitoring and regulating airport ground traffic to prevent or correct for runway incursions. The main overall functions of the proposed system would be to automatically monitor aircraft ground traffic on or approaching runways and to generate visible and/or audible warnings to affected pilots, ground-vehicle drivers, and control-tower personnel when runway incursions take place.

The system would include one or more portable units, denoted runway intersection display and monitor (RIDAM) units, that could be placed near taxiways. Each RIDAM unit would include an illuminated sign [and, optionally, a red ("stop") and a green ("go") traffic light mounted on top] that would be remotely controlled by means of encrypted signals transmitted from the control tower via a free-space or carrier-current radio-frequency (RF) link. The sign, lights, and associated communication and monitoring

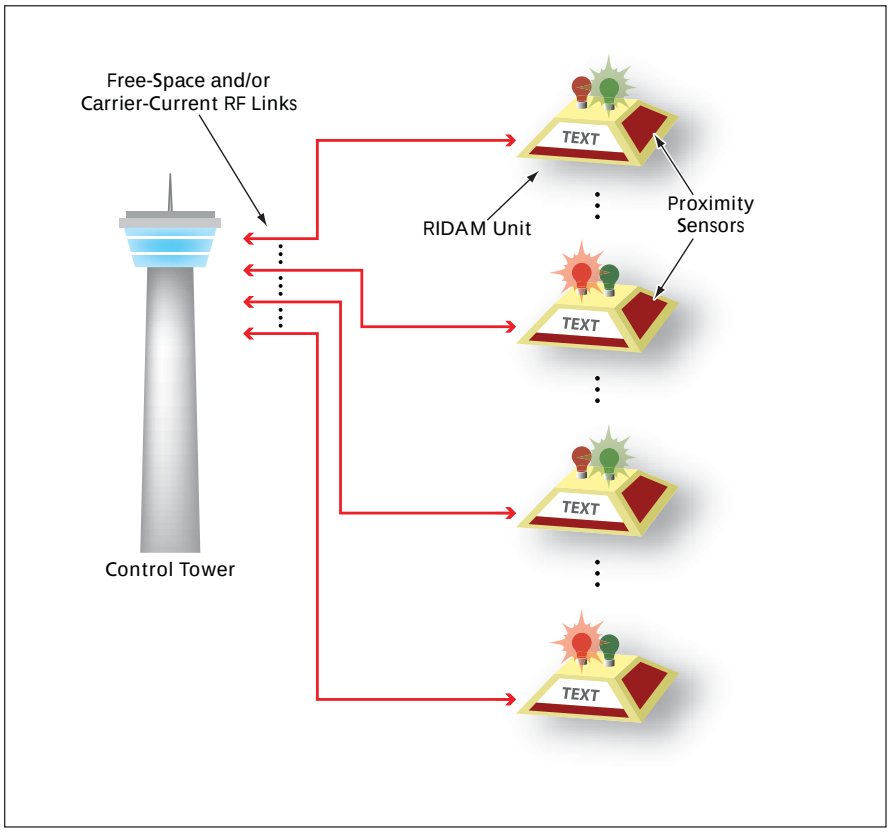

RIDAM Units placed alongside taxiways and runways would monitor aircraft moving on the ground, display short alphanumeric messages and go/stop commands from the control tower, and automatically issue warnings to pilots of aircraft moving in violation of runway clearances.

equipment could utilize solar power with battery backup. Alternatively or in addition, at night, power for operation and battery charging could be drawn from the power connection for pre-existing blue night taxiway lights. The system could readily be enhanced through addition of lights, signs, and other equipment at various taxiway and runway locations; this portability and enhanceability could be of great value during emergencies and airport modifications.

The illuminated sign could display stop/go signals or other short alphanumeric text messages to pilots of aircraft awaiting further clearance. The RIDAM unit would include one or more proximity sensors in the form of short-range radar, lidar, or video units that would generate movement-confirmation signals: that is, they would monitor positions of aircraft and ground vehicles and send information on those positions to the control tower. The RIDAM unit could include a transceiver that would interact with transponders on aircraft to identify or to confirm the identities of the aircraft. The RIDAM unit would periodically transmit, to the control tower, a "watchdog" signal, which would contain information on the statuses of the lights, sign, proximity sensor(s), and other components. A command processor in the RIDAM unit would automatically generate audible warnings to potential clearance violators and would both (1) broadcast the warnings locally via a short-range radio transmitter operating in a pre-existing aviation ground communication frequency band and (2) transmit the warnings to the control tower via the aforementioned free-space or carrier-current RF link.

This work was done by Richard Dabney and Susan Elrod of Marshall Space Flight Center.

This invention is owned by NASA, and a patent application has been filed. For further information, contact Sammy Nabors, MSFC Commercialization Assistance Lead, at sammy.a.nabors@nasa.gov. Refer to MFS-32307-1.

Smaller But Fully Functional Backshell for Cable Connector

Features include reduced size, shield termination, strain relief, and protection against EMI.

Lyndon B. Johnson Space Center, Houston, Texas

An improved design for the backshell of a connector for a shielded, multiple-wire cable reduces the size of the backshell, relative to traditional designs of backshells of otherwise identical cable connectors. Notwithstanding the reduction in size, the design provides all the functionality typically demanded of such a backshell, including (1) termination of the cable shield (that is, grounding of the shield to the backshell), (2) strain relief for the cable, and (3) protection against electromagnetic interference (EMI).

A traditional backshell design provides for termination of the cable shield inside the backshell. To accommodate the shield, the interior of the backshell must contain wasted volume and, consequently, must be larger than would otherwise be necessary. The present improved design provides for termination of the cable shield on the outside of the backshell, thereby eliminating the need for wasted interior volume and enabling a reduction in size. In particular, the backshell is now only about one-third as large as a corresponding traditional backshell.

As shown in the figure, the improved backshell includes a backshell body, a cover, and a band clamp. There is a hole in the backshell near its left (as shown in the figure) end to allow the cable shield to pass through to the outside of the backshell. The backshell body is fitted with a threaded coupling nut for securing this connector to a mating connector.

When the cover and the backshell are put together, lips in the form of mating corrugations along the edges of the cover and backshell help to prevent EMI by eliminating any straight path along which electromagnetic waves could penetrate to the cable wires. A male tab on the upper right corner of the backshell body mates with a female tab on the right end of the cover for latching the cover in

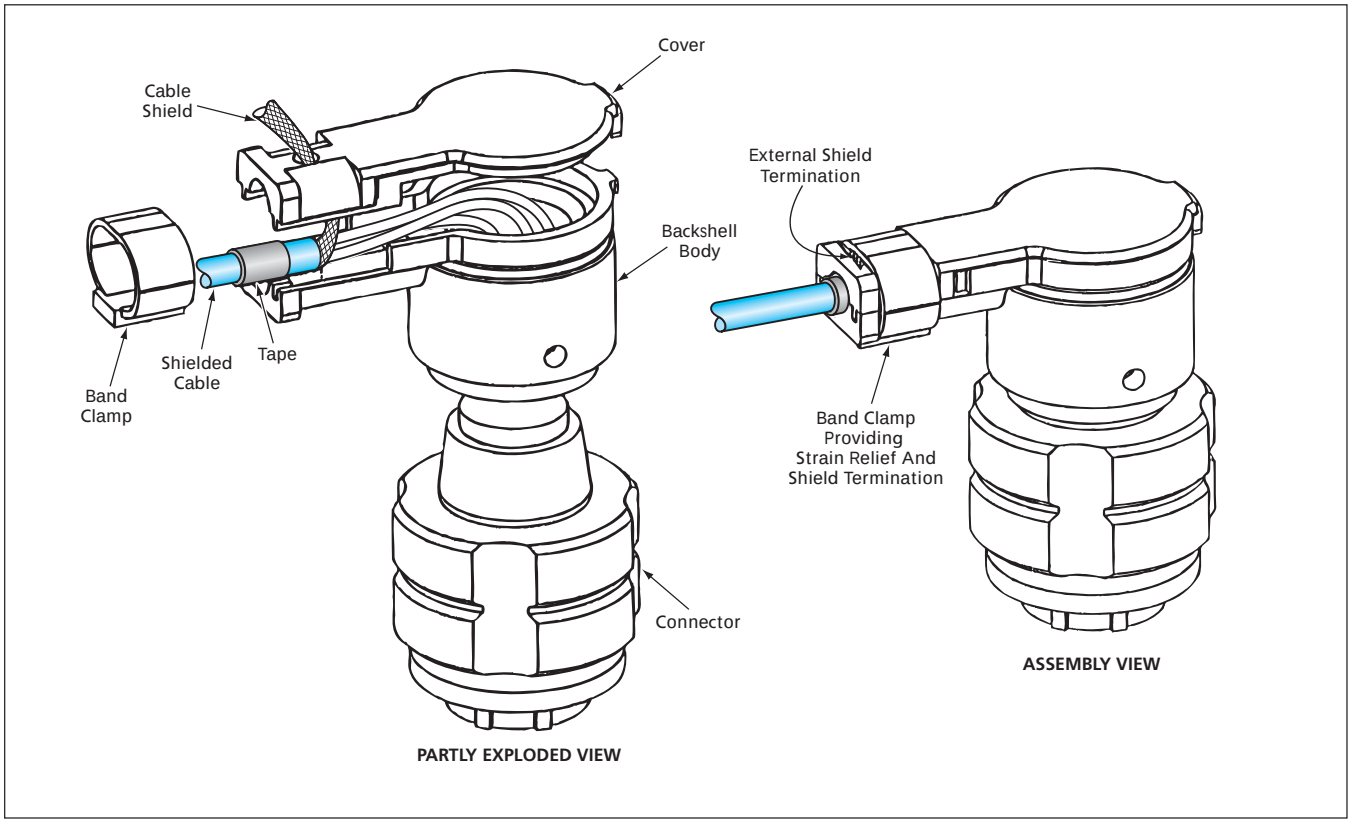

The **Cable Shield Is Terminated on the Outside** of the backshell instead of on the inside as in a traditional design. The mechanical and electrical integrity of the shield termination is ensured by squeezing of the shield between the cover and the band clamp.

place when the band clamp is tightened.

The procedure for assembling the cable, the backshell, and the rest of the connector is the following: The cable is placed through the coupling nut on the backshell body, the insulation on the cable wires is stripped back, and each wire is crimped to a connector pin. The pins are inserted in the connector. The coupling nut is threaded onto the connector. The shield (assumed to made of braided wire) pulled through the hole on the cover. Tape is wound around the cable near the left end of the backshell to provide strain relief. The cover is latched in place on the backshell body. The band clamp is tightened around the cover/backshell-body assembly with the shield squeezed between the cover and the band clamp. Once electrical continuity between the shield and the backshell has been verified, the shield is trimmed and the cable is examined for proper strain relief.

If the cable is unshielded or if termination of the shield is not needed, then except for omission of the steps involving the cable shield, the assembly procedure remains as described above. The design of the backshell for such a case can also remain the same, except that optionally, the hole near the left end of the cover can be eliminated because it is not needed.

This work was done by Chuong H. Diep of Hamilton Sundstrand Space Systems International, Inc. for Johnson Space Center.

Title to this invention, covered by U.S. Patent No. 7,044,795, has been waived under the provisions of the National Aeronautics and Space Act {42 U.S.C. 2457 (f)}. Inquiries concerning licenses for its commercial development should be addressed to:

Gregory Stephenson,
Assistant Intellectual Property Counsel
Hamilton Sundstrand
One Hamilton Road
Windsor Locks, CT 06096-1010

Refer to MSC-23670-1, volume and number of this NASA Tech Briefs *issue, and the page number.*

Glove-Box or Desktop Virtual-Reality System

Multiple remote users can participate in a realistic simulation of a work space.

Ames Research Center, Moffett Field, California

The figure depicts salient features of the optical layout of a desktop-scale virtual-reality system that is specialized for simulating a glove-box work space. The system generates stereoscopic left- and right-eye images of the interior of the work space that show (1) a user extension (defined here as an arm, hand, and/or one or more of the fingers on the hand of a user) and (2) either a real or a virtual workpiece to be manipulated by the user extension. The positions and orientations of the user extension and workpiece in the virtual images coincide substantially with those of the real user extension and of the real

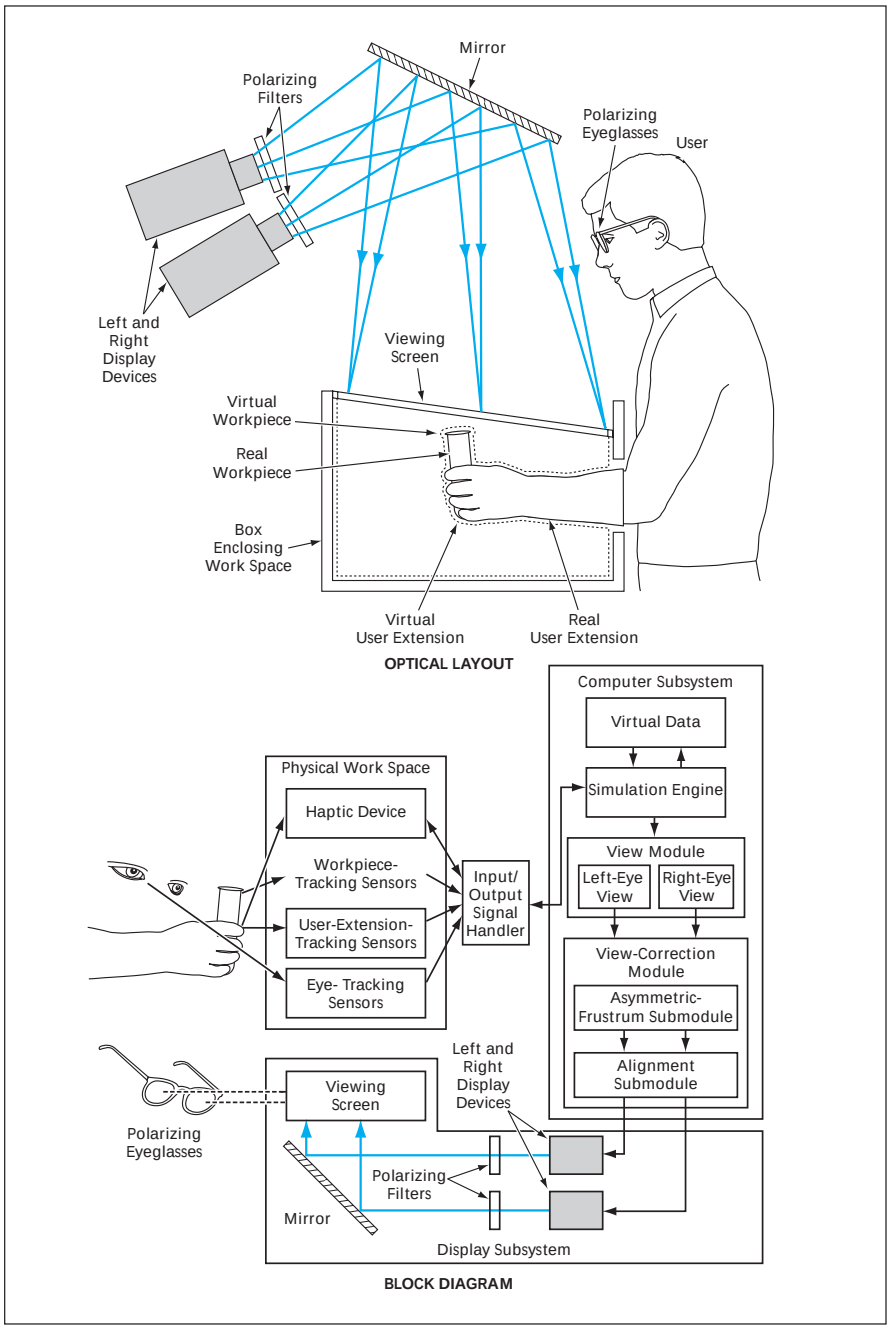

This **Virtual-Reality System** simulates a work space immediately in front of the user, as in a glove box. The system generates stereoscopic images that are compensated for changing positions of the user's eyes.

workpiece if one exists. The images are compensated for the non-central positions of the user's eyes relative to a viewing screen on which they are presented.

The system consists of three major parts: the physical work space, a computer subsystem, and a display subsystem. In addition to the user extension, the physical work space contains sensors that track the position and orientation of the user extension, sensors that track the positions of the user's eyes, and sensors that track the position and orientation of the workpiece (if any). Optionally, attached to the user extension is a pen-style haptic device — an assembly that can include actuators that apply forces to the end of a pen stylus held by a user to simulate contact between the stylus and a virtual workpiece. The sensor readings are digitized in real-time and sent to the computer subsystem.

The computer subsystem runs software, denoted a simulation engine, that simulates the manipulation of the workpiece by the user extension. The simulation engine includes mathematical models of all relevant aspects of the three-dimensional geometry and physical properties of the user extension and the workpiece, and calculates interactions between objects using a physics based force model. The simulation utilizes the tracking data provided by the sensors plus stored data (denoted virtual data) on the dimensions and physical properties of the user extension and the workpiece. The simulation can include such details as the positions and orientations of finger segments, contact forces with the stylus, and even deflections of the workpiece if the workpiece is a deformable body.

The output of the simulation engine is fed to a software module that generates nominal left- and right-eye views for eyes that are spaced apart by an amount that can be adjusted to match the interpupillary distance of the user. The views are then processed by a software module that uses the eye-tracking sensory data to correct for the deviation of the user's eye positions from nominal viewing positions. An important part of the view-correction module is a submodule in which the geometry of the viewing screen and the user's eyes is represented by means of an asymmetric frustum that is repeatedly updated in response to the eye-tracking data.

The outputs of the view-correction module are synchronized by an alignment submodule, then fed to the display subsystem, wherein two display devices generate the left- and right-eye images. The images are projected onto the viewing screen through circularly polarizing filters, such that the left and right images are polarized orthogonally to each other. The user wears a pair of correspondingly polarized eyeglasses so that the left or right eye sees only the left or right image, respectively.

A somewhat more complex version of the system can include two or more physical-work-space / display subsystem assemblies, possibly at different locations. The simulation engine from each work-space is connected via a network to the other simulation engines. This system would make it possible for multiple remote users to work together, or simulate working together, on the same workpiece.

This work was done by J. D. Smith and R. D. Boyle of Ames Research Center and I. Twombly of Universities Space Research.

This invention is owned by NASA and a patent application has been filed. Inquiries concerning rights for the commercial use of this invention should be addressed to the Ames Technology Partnerships Division at (650) 604-2954. Refer to ARC-14756-1.

Composite Layer Manufacturing With Fewer Interruptions

Lyndon B. Johnson Space Center, Houston, Texas

An improved version of composite layer manufacturing (CLM) has been invented. CLM is a type of solid freeform fabrication (SFF) — an automated process in which a three-dimensional object is built up, point-by-point, through extrusion of a matrix/fiber composite-material precursor. The elements of SFF include (1) preparing a matrix resin in a form in which it will solidify subsequently, (2) mixing fibers and matrix material to form a continuous preimpregnated tow (also called "towpreg"), and (3) dispensing the towpreg from a nozzle onto a base while moving the nozzle to form the dispensed material into a series of patterned layers of controlled thickness.

In CLM, the translation and the extrusion operation are such that the final size and shape of the fabricated object are as specified by a computer-aided design (CAD). Sometimes, in order to achieve the desired final shape, it is necessary to interrupt the deposition and cut the towpreg so that no material is deposited while the nozzle is translated to a position where deposition is to resume. The present improved version of CLM includes the use of an algorithm that generates a nozzle path with a minimum number of interruptions.

This work was done by Bor Z. Jang, Junhai Liu, and Shizu Chen of Auburn University for Johnson Space Center. For further information, contact the JSC Innovation Partnerships Office at (281) 483-3809.

In accordance with Public Law 96-517, the contractor has elected to retain title to this invention. Inquiries concerning rights for its commercial use should be addressed to:

Auburn University
Office of Technology Transfer
309 Samford Hall
Auburn University, Al 36849-5176
Phone No.: (334) 844-4977
Fax No.: (334) 844-5963
E-mail: ott@auburn.edu

Refer to MSC-23452-1, volume and number of this NASA Tech Briefs *issue, and the page number.*

Improved Photoresist Coating for Making CNT Field Emitters

This technique could contribute to development of cold cathodes for diverse applications.

NASA's Jet Propulsion Laboratory, Pasadena, California

An improved photoresist-coating technique has been developed for use in the fabrication of carbon-nanotube- (CNT)-based field emitters of the type described in "Fabrication of Improved Carbon-Nanotube Field Emitters" (NPO-44996), *NASA Tech Briefs*, Vol. 32, No. 4 (April 2008), page 50. The improved photoresist-coating technique overcomes what, heretofore, has been a major difficulty in the fabrication process. This technique is expected to contribute to the realization of high-efficiency field emitters (cold cathodes) for diverse systems and devices that could include gas-ionization systems, klystrons, flat-panel display devices, cathode-ray tubes, scanning electron microscopes, and x-ray tubes.

To recapitulate from the cited prior article: One major element of the device design is to use a planar array of bundles of carbon nanotubes as the field-emission tips and to optimize the critical dimensions of the array (principally,

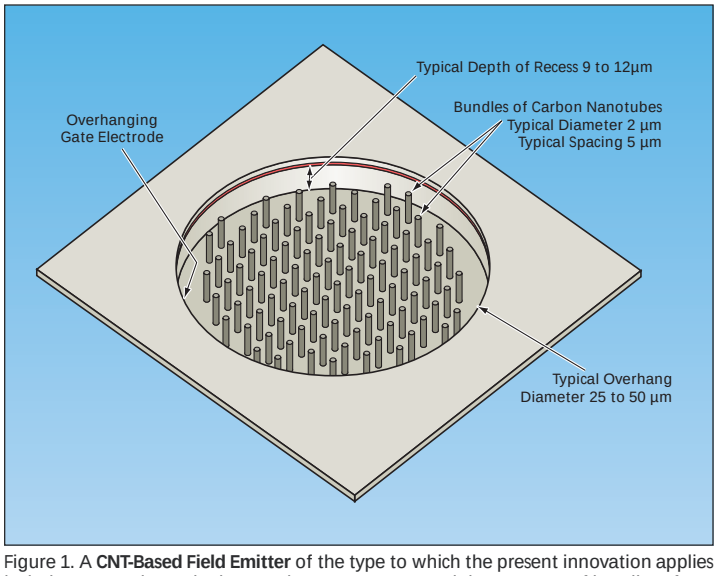

Figure 1. A **CNT-Based Field Emitter** of the type to which the present innovation applies includes a gate electrode that overhangs a recess containing an array of bundles of carbon nanotubes. For the sake of clarity, this drawing is simplified and not to scale.

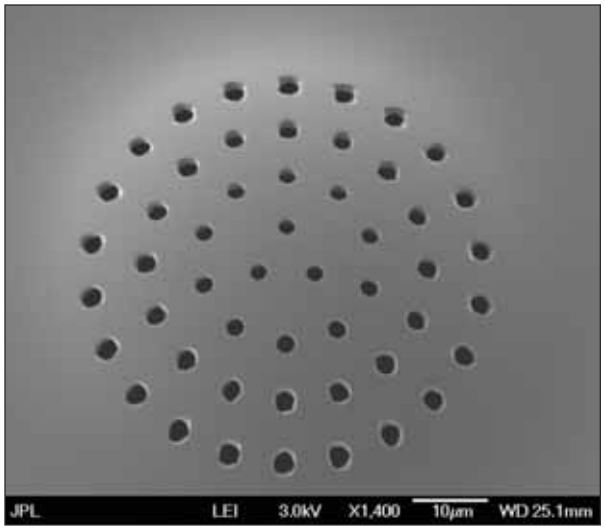

Figure 2. **Holes To Define Catalyst Dots** were formed in a photoresist membrane bridging a recess like that of Figure 1. This scanning electron micrograph was recorded at tilt angle of 20° to make the slight bulge of the membrane more visible.

heights of bundles and distances between them) to obtain high area-averaged current density and high reliability over a long operational lifetime. Another major element of the design is to configure the gate electrode (an anode used to generate the electron-emitting and -accelerating electric field) as a ring that overhangs a recess wherein the bundles of nanotubes are located (see Figure 1), such that by virtue of the proximity between the ring and the bundles, a relatively low applied potential suffices to generate the large electric field needed for emission of electrons.

The major difficulty in the fabrication process as practiced before the development of the improved photoresist-coating technique arises in the step immediately after the formation of the overhang and the recess. In this step, it is necessary to spin-coat the flat bottom surface of the recess with a uniform layer of a photoresist that is to be patterned with holes in a subsequent photolithographic step. The patterned photoresist is then to be used in subsequent deposition and liftoff steps to form dots of a catalytic material, about 2 μm in diameter and spaced about 5 μm apart, upon which the bundles of CNTs are to be grown. The difficulty is caused by a combination of the dimensions of the recess and overhang, the surface tension and viscosity of the photoresist solution, and the centrifugal force associated with spin coating. The net effect is that it becomes difficult or impossible to make the photoresist solution flow into or out of the recess and, hence, difficult or impossible to coat the bottom of the recess to the required uniform thickness. Often, the photoresist solution bridges over the recess.

The concept underlying the improved photoresist-coating technique is to turn the source of difficulty to advantage. In this technique, one does not attempt to make the photoresist solution flow into the recess: Instead, the photoresist solution and spin-coating conditions are chosen to maximize the tendency of the photoresist solution to become formed into a uniform-thickness membrane bridge over the recess. After spin coating, the workpiece is subjected to a soft bake in which the air trapped in the recess expands, causing the photoresist membrane to acquire an outward bulge between 5 and 10 μm. The bake solidifies the membrane, which thereafter retains the bulge. Then the pattern of holes is formed on the photoresist membrane bridge (see Figure 2). Experiments have confirmed that the patterned membrane bridge can be used to form the corresponding pattern of dots of catalytic material on the flat bottom surface of the recess and that the bundles of carbon nanotubes can be grown on these dots.

This work was done by Risaku Toda and Harish Manohara of Caltech for NASA's Jet Propulsion Laboratory.

In accordance with Public Law 96-517, the contractor has elected to retain title to this invention. Inquiries concerning rights for its commercial use should be addressed to:

Innovative Technology Assets Management
JPL
Mail Stop 202-233
4800 Oak Grove Drive
Pasadena, CA 91109-8099
E-mail: iaoffice@jpl.nasa.gov

Refer to NPO-45624, volume and number of this NASA Tech Briefs *issue, and the page number.*

A Simplified Diagnostic Method for Elastomer Bond Durability

Less time and equipment are needed.

NASA's Jet Propulsion Laboratory, Pasadena, California

A simplified method has been developed for determining bond durability under exposure to water or high humidity conditions. It uses a small number of test specimens with relatively short times of water exposure at elevated temperature. The method is also gravimetric; the only equipment being required is an oven, specimen jars, and a conventional laboratory balance.

Elastomers (rubbers) are frequently bonded to other surfaces, including glasses, metals, and occasionally other polymers. Due to mismatches in chemistry, thermal expansion and stiffness, the bonded interfaces usually require the use of a primer. Initial bond strengths can be determined by tensile testing, but the long-term durability of these bonds is uncertain, as is the effectiveness of the primer. This is especially the case when these bonds are exposed to humidity, thermal cycling, and possibly ultraviolet light.

Decline in bond strength is usually due to the intrusion of water at the bond interface. Water may chemically attack the primer chemistry, draw ions out from the glass or metal surface, and add stress from expansion. The long-term stability of bonded elastomers in humid environments is difficult to determine without very large numbers of test specimens and very long periods of water exposure.

A new method for determining rubber/glass bond durability was devised in which finely divided substrate (glass beads) was dispersed in the elastomer and the amount of absorbed water measured by weight gain. The difference between primed and unprimed glass beads was immediately apparent, and the stability of the bond was determined by measuring the time to a sudden increase in weight gain.

The materials used in this study were: (a) EVA; an elastomer of ethylene-vinyl acetate (33 percent) copolymer, (b) spherical glass micro-beads as the substrate, and (c) a primer consisting of methacryloxy propyl trimethoxy silane. The glass microbeads had an average diameter of 30 microns, and were primed with 5 percent by weight of the primer deposited from an alcohol solution. The test specimens were made by blending 30 percent by volume of the glass beads (primed and unprimed) into the EVA polymer with the use of a two-roll differential mill, while adding 1.5 percent of a curing (vulcanizing) agent. A heat-activated peroxide agent was used [t-Butyl-O-(2-ethylhexyl)monoperoxy carbonate]. Compounded specimens were compression molded into sheets of 0.060-in. (1.52-mm) thickness, and cured at 150 °C for 30 minutes. The curing process vulcanizes the EVA rubber and also activates the primer to create a strong bond to the glass surface.

Table 1 provides strength and weight gain data for primed and unprimed

Temperature°C		40	40	60	60	60	80	80	80
UNPRIMED (Hrs)	**Control**	**500**	**2,000**	**250**	**500**	**2,000**	**250**	**500**	**1,000**
Strength,psi	1,380	1,230	1,210	960	530	50	285	310	0
Elongation,%	600	570	510	515	300	60	120	100	0
Weight gain, %	---	19	51	29	410	2,015	568	503	0
PRIMED (Hrs)	**Control**	**500**	**2,000**	**250**	**500**	**2,000**	**250**	**500**	**1,000**
Strength,psi	905	900	1,150	930	990	830	1,010	910	725
Elongation, %	350	190	390	285	315	120	245	220	140
Weight gain, %	---	2	4	4	6	35	13	17	62

Table 1. **Water Gain and Strength** are shown for EVA rubber containing primed and unprimed glass beads

Temperature°C		40	40	60	60	60	80	80	80
UNPRIMED (Hrs)	**Control**	**500**	**2,000**	**250**	**500**	**2,000**	**250**	**500**	**1,000**
Strength,psi	1,380	1,280	1,210	1,340	960	480	560	0	0
Elongation,%	600	565	570	575	500	280	290	0	0
Absorbed water,%	0	0	0	0	0	0	0	0	0
PRIMED (Hrs)	**Control**	**500**	**2,000**	**250**	**500**	**2,000**	**250**	**500**	**1,000**
Strength,psi	905	990	860	890	980	850	920	920	880
Elongation, %	350	315	260	240	240	240	310	310	260
Absorbed water, %	0	0	0	0	0	0	0	0	0

Table 2. **Recovery of Water-Exposed Specimens** is shown for primed and unprimed cases.

specimens after water immersion at 40, 60, and 80 °C. Cured EVA rubber containing no glass beads gained only 1 weight percent water. This shows that the immense weight gain of other specimens is due to water absorption at the glass/elastomer interface. This was also verified by FTIR (Fourier Transform Infrared) spectroscopy.

The amount of water absorption in specimens containing glass beads is dramatically changed by the presence of the primer, particularly in the specimens immersed in water at the 80 °C temperature. Unprimed specimens aged in water at 60 °C for 2,000 hours showed a 2015-percent increase in weight, whereas primed glass bead specimens gained only 35 percent. Reduction in tensile strength also followed primed and unprimed specimens, and increasing exposure times and temperatures.

Importantly, this method can provide semi-quantitative measurement of the bond resistance to water by measuring the time to the sudden increase in weight. This effect is due to degradation of the primer chemistry at the interface. The longer the time to weight increase, the more effective is the primer and the more water resistant is its chemical bond.

Duplicate specimens of those reported in the first table were dried to constant weight and retested for tensile strength. This was done to determine the recoverability of hydrothermal attack after water removal. Specimens containing primed glass microbeads recovered their initial properties almost entirely, whereas the unprimed glass beads, especially in the 80 °C water exposure, deteriorated too badly to be tested.

Table 2 presents the results as percentage retention of control values: This method offers a simplified way of (a) determining the effectiveness of primers used for bonding elastomers to glass, and perhaps other substrates, in environments with humidity or water exposure; (b) a semi-quantitative technique for determining bond stability; and (c) a method for determining the long term durability and onset of hydrolytic attack at the interface. This method has the advantages of requiring very few specimens and only a laboratory balance to perform measurements.

This work was done by Paul White of Caltech for NASA's Jet Propulsion Laboratory. Further information is contained in a TSP (see page 1). ***NPO-43912***

Complex Multifunctional Polymer/Carbon-Nanotube Composites

CNTs are treated and incorporated into composites to obtain enhanced properties.

Marshall Space Flight Center, Alabama

A methodology for developing complex multifunctional materials that consist of or contain polymer/carbon-nanotube composites has been conceived. As used here, "multifunctional" signifies having additional and/or enhanced physical properties that polymers or polymer-matrix composites would not ordinarily be expected to have. Such properties include useful amounts of electrical conductivity, increased thermal conductivity, and/or increased strength. In the present methodology, these properties are imparted to a given composite through the choice and processing of its polymeric and CNT constituents.

The methodology involves utilization of CNTs in any or all of several ways:

- Coating the CNTs to impart desired properties — for example, coating them with electrically and/or thermally conductive polymers, which could be dissolved in solvents;
- Incorporating uncoated or coated CNTs into a polymeric matrix, possibly in such a manner as to improve the properties of the CNTs, the matrix, and/or the resulting composite; and/or
- Using a polymer/CNT composite as the matrix ingredient of a complex composite that includes any of a variety of other fibrous reinforcing materials.

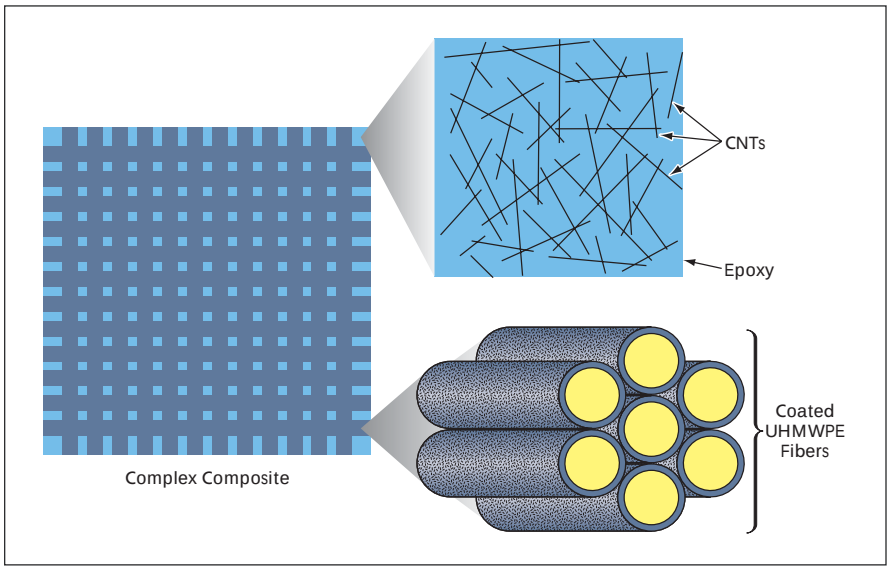

This **Complex Composite** consists of a fabric of coated UHMWPE fibers in a matrix material consisting of an epoxy/CNT composite.

The figure is a simplified illustration of an example of such a complex composite. In this case, a fabric made of coated ultra-high-molecular-weight polyethylene (UHMWPE) fibers is embedded in a matrix that is, itself, a composite of CNTs in an epoxy matrix. Typically, heretofore, such a composite would be designed and fabricated to obtain high strength, would not contain CNTs, and would be electrically insulating and, to some extent, thermally insulating. By incorporating a suitable quantity of CNTs, one can obtain enough electrical conductivity to drain off excess static electricity to prevent static discharge or to render the composite effective as a barrier against electromagnetic interference, and to obtain usefully large degrees of thermal conductivity and thermal stability, all without sacrificing mechanical strength.

This work was done by Pritesh Patel, Gobinath Balasubramaniyam, and Jian Chen of Zyvex Corp. for Marshall Space Flight Center. For further information, contact Sammy Nabors, MSFC Commercialization Assistance Lead, at sammy.a.nabors@nasa.gov. Refer to MFS-32355-1.

Very High Output Thermoelectric Devices Based on ITO Nanocomposites

Thermocouples based on this material perform better than precious-metal thermocouples.

John H. Glenn Research Center, Cleveland, Ohio

A material having useful thermoelectric properties was synthesized by combining indium-tin-oxide (ITO) with a NiCoCrAlY alloy/alumina cermet. This material had a very large Seebeck coefficient with electromotive-force-versus-temperature behavior that is considered to be excellent with respect to utility in thermocouples and other thermoelectric devices. When deposited in thin-film form, ceramic thermocouples offer advantages over precious-metal (based, variously, on platinum or rhodium) thermocouples that are typically used in gas turbines. Ceramic thermocouples exhibit high melting temperatures, chemical stability at high temperatures, and little or no electromigration. Oxide ceramics also resist oxidation better than metal thermocouples, cost substantially less than precious-metal thermocouples, and, unlike precious-metal thermocouples, do not exert catalytic effects.

Ceramic thermocouples based on the present indium-tin-oxide/(NiCoCrAlY-alloy/alumina nanocomposite) combination were demonstrated at temperatures up to 1,200 °C. An SEM (scanning electron microscope) micrograph of the starting NiCoCrAlY-alloy/alumina composite material and resulting NiCoCrAlY-alloy/alumina nanocomposite produced by sputtering is shown in the figure.

In other tests, thin-film thermocouples were synthesized by directly combining indium-tin-oxide and a NiCoCrAlY alloy at small length scales to form "n-type" and "p-type" nanocomposites. These indium-tin-oxide/NiCoCrAlY nanocomposites exhibited extremely large and stable Seebeck coefficients (S> 2000 μV/K) when thermally cycled between room temperature and 1,500 °C. From observations made in these tests, it was concluded that the sensitivity and other aspects of performance of these thermocouples are large enough to be considered for energy harvesting applications and superior to those of precious-metal thermocouples.

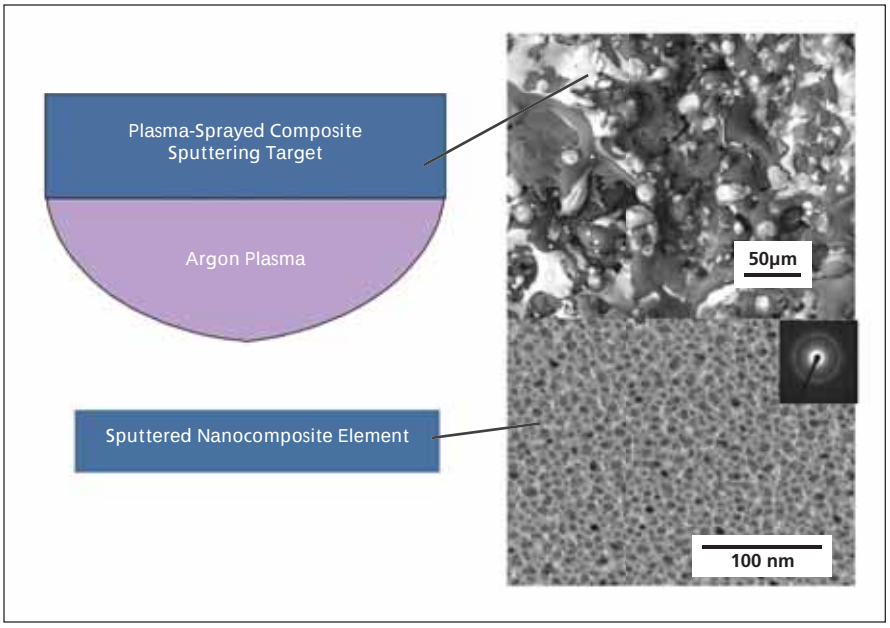

SEM Micrograph is shown of the starting NiCoCrAlY-alloy/alumina composite material and resulting NiCoCrAlY-alloy/alumina nanocomposite produced by sputtering. Note the distribution of phases at small length scales in the nanocomposite (TEM in lower right).

This work was done by Otto J. Gregory of the University of Rhode Island and Gustave Fralick of the Glenn Research Center.

Inquiries concerning rights for the commercial use of this invention should be addressed to NASA Glenn Research Center, Innovative Partnerships Office, Attn: Steve Fedor, Mail Stop 4–8, 21000 Brookpark Road, Cleveland, Ohio 44135. Refer to LEW-18120-1.

Reducing Unsteady Loads on a Piggyback Miniature Submarine

Simple, highly effective fixtures entail minimal modification.

Langley Research Center, Hampton, Virginia

A small, simple fixture has been found to be highly effective in reducing destructive unsteady hydrodynamic loads on a miniature submarine that is attached in piggyback fashion to the top of a larger, nuclear-powered, host submarine (see Figure 1). The fixture, denoted compact ramp, can be installed with minimal structural modification, and the use of it does not entail any change in submarine operations.

The miniature submarine is denoted as Advanced SEAL Delivery System [ASDS (wherein "SEAL" signifies the United States Navy's special-operations forces known as the Sea, Air and Land (SEAL) forces.] The ASDS is launched from the host submarine to clandestinely transport a SEAL team to a landing site, where the team performs an operation. Later, the ASDS is used to return the SEAL team to the host submarine.

During sea trials and subsequent computational analysis, large unsteady hydrodynamic loads were detected on the stern of the ASDS during piggyback transport. It was discovered that the unsteady hydrodynamic forces and moments were associated with unsteady separated flow that was caused by the combination of a strong adverse pressure gradient on the stern of the ASDS as well as blockage of flow by a mating trunk, pylon fairings, pylon cross struts, latches, and other fixtures used for mounting the ASDS on the host submarine. The unsteady loads acted on the rudders, stern planes, propeller, stators, and stern cone of the ASDS, causing fatigue and early failure of critical components.

An investigation of flow-control modifications to reduce the unsteady hydrodynamic loads was initiated. Of thirty modifications that were considered, the one judged to be most promising was the installation of a compact ramp on the host submarine hull between the rear ends of the aft pylon pair, near the stern of the ASDS. Unlike other flow-control modifications examined, this one is not based on the concept of confronting and reducing the flow separation directly; instead, it is based on the concept of mitigating the ad-

Figure 1. A **Miniature Submarine**, denoted an ASDS as explained in the text, rides piggyback on a submarine of the Los Angeles class.

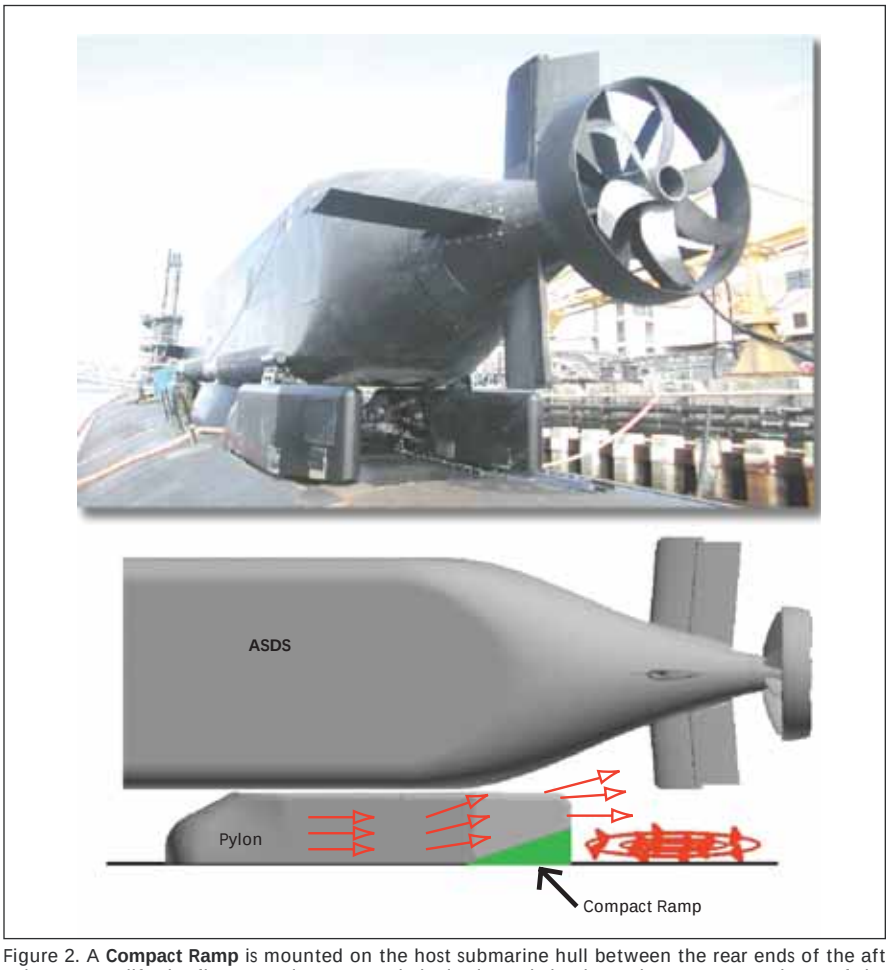

Figure 2. A **Compact Ramp** is mounted on the host submarine hull between the rear ends of the aft pylons to modify the flow to reduce unsteady hydrodynamic loads on the stern appendages of the ASDS.

verse pressure gradient and moving the flow separation away from the critical stern components of the ASDS and harmlessly onto the host hull downstream of the ramp, as depicted schematically in the lower part of Figure 2.

In water-tunnel tests on a scale model, the installation of the compact ramp was found to result in reductions of as much as 50 percent in unsteady hydrodynamic forces and moments on the stern appendages of the ASDS, leading to the selection of the compact ramp as sole candidate recommended for testing in full-scale sea trials. It has also been conjectured that structural components similar to the compact ramp could, potentially, confer flow-control and load-reduction benefits in applications that involve piggyback or other external attachments to aircraft.

This work was done by John Lin of Langley Research Center. Further information is contained in a TSP (see page 1). ***LAR-17364-1***

Ultrasonic/Sonic Anchor

The anchor can be embedded or de-embedded with minimal axial force.

NASA's Jet Propulsion Laboratory, Pasadena, California

The ultrasonic/sonic anchor (U/S anchor) is an anchoring device that drills a hole for itself in rock, concrete, or other similar material. The U/S anchor is a recent addition to a series of related devices, the first of which were reported in "Ultrasonic/Sonic Drill/Corers With Integrated Sensors" (NPO-20856), *NASA Tech Briefs*, Vol. 25, No. 1 (January 2003), page 38. There are numerous potential uses for U/S anchors, especially in enabling walking robots and humans to climb steep rock faces for diverse purposes, including scientific exploration, recreational rock climbing, military maneuvers, and search and rescue.

Like the prior devices in this series, the U/S anchor drills a hole by means of hammering and chiseling actions of a tool bit excited with a combination of ultrasonic and sonic vibrations. The U/S anchor also contains an actuator that includes a piezoelectric stack at the upper end of a rodlike horn that serves to mechanically amplify the piezoelectric displacement. In addition, as in the previously related devices, the tool bit is mounted at the lower end of the horn. The piezoelectric stack is electrically driven at its resonance frequency (an ultrasonic frequency), and a bolt holds the stack in compression to prevent fracture during operation.

In a typical prior related device, the sonic vibrations are generated with the help of upper and lower mass that is denoted the free mass because it is free to move axially through a limited range within the actuator/tool-bit assembly. In the U/S anchor, there are two free masses: one above and one below the lower tip of the horn (see figure). Each free mass bounces between hard stops at the limits of its range of motion at a sonic frequency. The impacts of the free masses on the hard stops create stress pulses that propagate along the horn, to and through the tool bit, to the tool-bit/rock interface. The rock becomes fractured when its ultimate strain is exceeded.

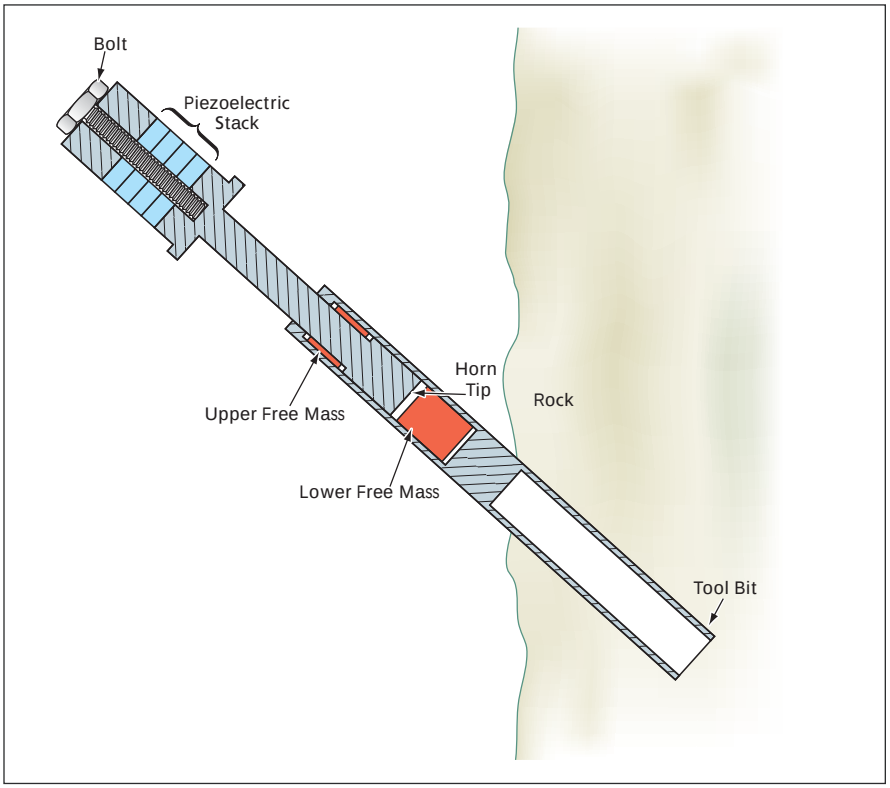

The **Ultrasonic/Sonic Anchor** drills its own anchor hole in a rock face.

A major advantage of the U/S anchor (or of any device in this series) is that it is not necessary to apply a large axial force to make the tool bit advance into the drilled material. Similarly, during operation, only a small force suffices to extract the tool bit from the drilled hole. Hence, a human or robotic rock climber could easily insert and withdraw a U/S anchor at successive positions during traversal of a rock face.

This work was done by Yoseph Bar-Cohen and Stewart Sherrit of Caltech for NASA's Jet Propulsion Laboratory. Further information is contained in a TSP (see page 1).

This invention is owned by NASA, and a patent application has been filed. Inquiries concerning nonexclusive or exclusive license for its commercial development should be addressed to the Patent Counsel, NASA Management Office–JPL. Refer to NPO-40827.

Grooved Fuel Rings for Nuclear Thermal Rocket Engines

Improvements in performance, fabrication, and reliability are anticipated.

Marshall Space Flight Center, Alabama

An alternative design concept for nuclear thermal rocket engines for interplanetary spacecraft calls for the use of grooved-ring fuel elements. Beyond spacecraft rocket engines, this concept also has potential for the design of terrestrial and spacecraft nuclear electric-power plants.

Nuclear thermal rocket engines can produce high thrusts at specific impulses at least twice those of today's best chemical rocket engines. In a nuclear thermal rocket engine, a nuclear reactor is used to heat hydrogen propellant to high temperatures. The resulting expansion and expulsion of the hydrogen exhaust through a nozzle produces thrust. The performance of nuclear engines is restricted primarily by the limited ability of the nuclear fuel to withstand the extremely high operating temperatures and by the corrosive effects of the hot hydrogen propellant.

The grooved ring fuel element design addresses some of the problems encountered with an alternate fuel design concept used in the Particle Bed Reactor (PBR). In the PBR, the fuel element consists of two concentric porous pipes (called frits) in between which is supported a bed of tiny fuel particles. Hydrogen propellant flows through the walls of the outer cold frit, through the fuel particle bed where it was heated to high temperatures, and finally exits through the walls of the inner hot frit. The propellant then leaves the fuel element through the central cavity where it is expelled through a nozzle. Because of the high surface-to-volume ratio of the fuel particles in the PBR concept, extremely high heat transfer rates were thought possible, which, had the concept proved successful, would have resulted in a very compact reactor with a high thrust-to-weight ratio. Unfortunately, because the particle bed design does not constrain the hydrogen propellant to following well-defined flow paths, the fuel element proved to be thermally unstable. This instability was manifest during testing by the appearance of potentially dangerous local hot spots within the fuel bed.

The grooved ring fuel design attempts to retain the best features of the particle bed fuel element while eliminating most of its design deficiencies. In the grooved ring design, the hydrogen propellant enters the fuel element in a manner similar to that of the PBR fuel element. Once inside the fuel element, however, the hydrogen propellant enters a stack of fuel rings rather than a bed of fuel particles. The hydrogen propellant flows radially along the grooved faces of the individual fuel rings, finally exiting into the central cavity where it is expelled from the fuel element. The fuel rings are held in place by a hexagonal structure, which may or may not contain moderating material, depending upon whether the reactor is designed to be a fast reactor or a thermal reactor.

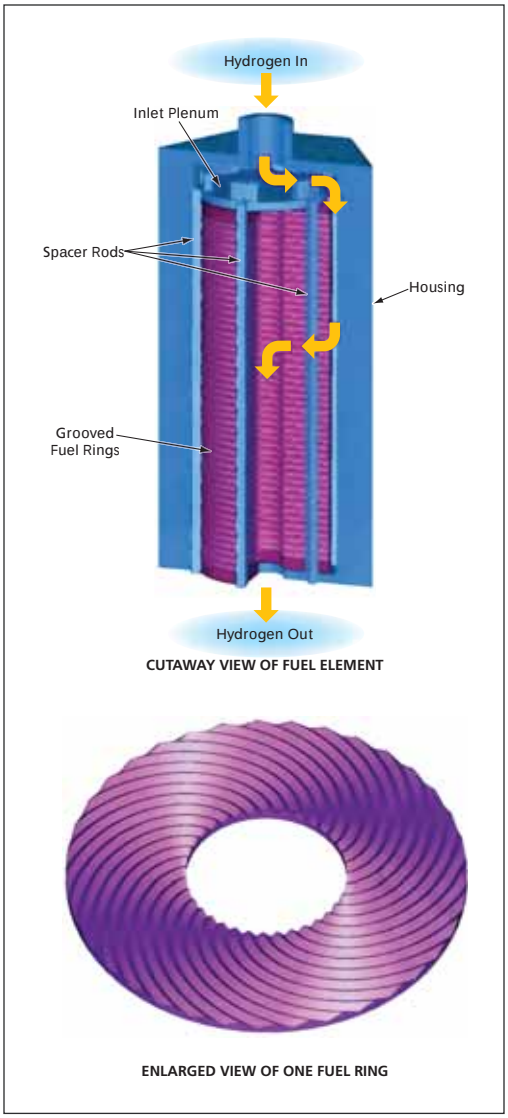

A **Fuel Element** as proposed would contain grooved fuel rings. The grooves would constitute well-defined flow paths that could be shaped to optimize flow and heat-transfer characteristics.

The advantages of this design concept include the following:

- The surface-to-volume ratios of the grooved fuel rings should approach that of particle-bed reactors, thus permitting the high heat-transfer rates, which would allow the design of compact reactors with high thrust-to-weight ratios.
- Unlike the particle bed reactor fuel element design, the grooved surface of the fuel rings offers well-defined flow paths for the hydrogen propellant, thus permitting the control of thermal instabilities.
- The cross-sectional areas of these flow paths may be optimized so as to meet a desired set of thermal hydraulic parameters.
- The grooved fuel ring design eliminates the need for the difficult-to-construct and prone-to-failure hot and cold frits required by the particle bed fuel element configuration.

The grooved fuel rings should be relatively easy to fabricate using such straightforward techniques as pressing and sintering. This ease of fabrication should allow fuel elements to be made of fairly exotic high-performance materials such as uranium tricarbide, which is generally quite difficult to work with under normal circumstances.

This work was done by William (Bill) Emrich of Marshall Space Flight Center.

This invention is owned by NASA, and a patent application has been filed. For further information, contact Sammy Nabors, MSFC Commercialization Assistance Lead, at sammy.a.nabors@nasa.gov. Refer to MFS-32342-1.

Pulsed Operation of an Ion Accelerator

Thrust can be varied more rapidly and with greater precision and range.

NASA's Jet Propulsion Laboratory, Pasadena, California

Electronic circuitry has been devised to enable operation of an ion accelerator in either a continuous mode or a high-peak-power, low-average-power pulsed mode. In the original intended application, the ion accelerator would be used as a spacecraft thruster and the pulse mode would serve to generate small increments of impulse for precise control of trajectories and attitude. On Earth, pulsed operation of ion accelerators could be utilized to effect precise control of output ion fluxes in plasma and ion-beam apparatuses commonly used in the semiconductor processing industry.

It has been conventional practice to operate an ion thruster in a continuous mode in which (1) the thrust or ion flux is regulated by adjustment of the discharge current and/or throttling of the gas from which the ions are formed and (2) the extraction voltage (typically of the order of a kilovolt) is maintained constant or adjusted over a limited range. These techniques produce only a limited range of the average thrust and the control subsystem needed for upstream regulation of thrust or ion flux is necessarily somewhat complex.

The present electronic drive circuitry generates the extraction voltage in pulses. Pulse-width modulation can affect rapid, fine control of time-averaged impulse or ion flux down to a minimum level much lower than that achievable in continuous operation (see figure). Since there is little or no need for upstream regulation to affect fine control, the upstream operational parameters can be held constant and, therefore, much of the control subsystem heretofore needed for upstream regulation can be simplified.

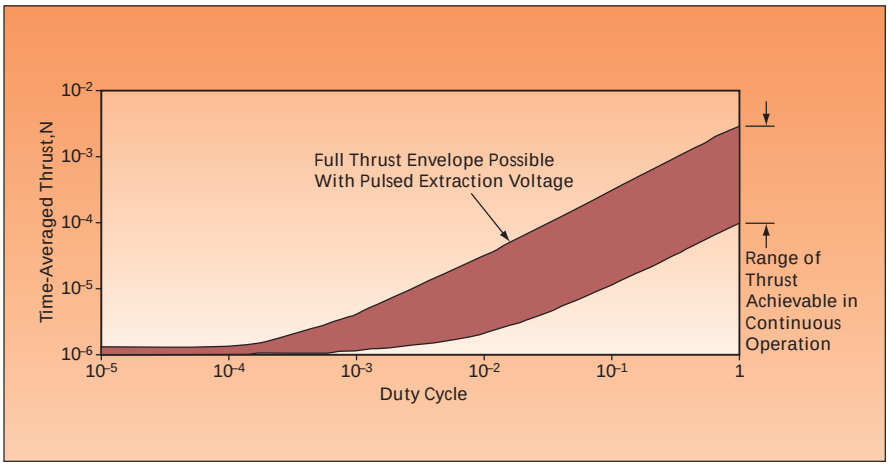

Time-Averaged Thrust was calculated theoretically for a representative ion thruster operating in continuous and pulse modes. A minimum average thrust much lower than that attainable in continuous operation (about 1 μN, below which the thrust due to ion flux is comparable to the flow of the propellant gas without ionization) would be achieved by pulsing at a low duty cycle.

The challenge in designing the circuitry was to provide rapid turn-on and turn-off of the high extraction voltage in the presence of thruster and circuit capacitances, while preventing undesired voltage and current transients. The approach taken to meet this challenge was to utilize a low-voltage pulsed waveform from a signal generator to command a pulse-circuit to generate a corresponding high-voltage waveform, and to enable rapid bleeding of charge from the high-voltage side of the thruster capacitance to thruster common (that is, thruster ground) when the high-voltage pulse is turned off. The signal generator drives an operational amplifier that triggers a transistor, the output of which causes the simultaneous opening and closing of the various thruster voltage lines. One of the lines contains an appropriately sized resistor that serves to drain the thruster capacitance to achieve rapid fall of the voltage and current, and thereby the thrust, which allows very precise thrust knowledge and minimizes thruster erosion, while preventing ground loops.

This work was done by Richard Wirz, Manuel Gamero-Castaño, and Dan Goebel of Caltech for NASA's Jet Propulsion Laboratory.

In accordance with Public Law 96-517, the contractor has elected to retain title to this invention. Inquiries concerning rights for its commercial use should be addressed to:

Innovative Technology Assets Management
JPL
Mail Stop 202-233
4800 Oak Grove Drive
Pasadena, CA 91109-8099
E-mail: iaoffice@jpl.nasa.gov

Refer to NPO-44961, volume and number of this NASA Tech Briefs *issue, and the page number.*

Software

Autonomous Instrument Placement for Mars Exploration Rovers

Autonomous Instrument Placement (AutoPlace) is onboard software that enables a Mars Exploration Rover to act autonomously in using its manipulator to place scientific instruments on or near designated rock and soil targets. Prior to the development of AutoPlace, it was necessary for human operators on Earth to plan every motion of the manipulator arm in a time-consuming process that included downlinking of images from the rover, analysis of images and creation of commands, and uplinking of commands to the rover. AutoPlace incorporates image analysis and planning algorithms into the onboard rover software, eliminating the need for the downlink/uplink command cycle. Many of these algorithms are derived from the existing ground-based image analysis and planning algorithms, with modifications and augmentations for onboard use.

AutoPlace also utilizes pre-existing onboard arm control, arm collision-detection, and stereoscopic image processing software. In addition, to satisfy needs specific to the Mars Exploration Rovers and to increase safety, AutoPlace incorporates a volumetric terrain visibility analysis algorithm, a uniform target selection algorithm, and a template-based trajectory generation algorithm that were not parts of the prior onboard or ground software.

This program was written by P. Chris Leger and Mark Maimone of Caltech for NASA's Jet Propulsion Laboratory. Further information is contained in a TSP (see page 1).

This software is available for commercial licensing. Please contact Karina Edmonds of the California Institute of Technology at (626) 395-2322. Refer to NPO-44820.

Mission and Assets Database

Mission and Assets Database (MADB) Version 1.0 is an SQL database system with a Web user interface to centralize information. The database stores flight project support resource requirements, view periods, antenna information, schedule, and forecast results for use in mid-range and long-term planning of Deep Space Network (DSN) assets.

Project requirements can be entered using interval-based patterns, which allow planning analysts to capture project requirements more accurately. Project information can be stored in such a way as to allow multiple sets to be entered for various scenario studies. For example, a mission can have multiple view periods and many sets of requirements. This extends to schedules and forecasts as well. The Web component of this system allows users to modify this information and to generate graphical and tabular reports from it.

Unlike other toolsets used previously, MADB allows the user to enter requirements in the most flexible way. It also allows for many view periods for each project as well as a hierarchy system for classifying them. MADB-generated reports can span multiple projects and view periods. MADB uses an industry-standard SQL database, which enables future generic software improvement and multiple levels of access. The Web interface also can be accessed from any platform.

The RAPS TIGRAS and DRAGON tools are tightly integrated with MADB. Together they are used by the Resource Allocation Planning Service to schedule and forecast DSN assets.

This program was written by John Baldwin, Silvino Zendejas, Sandy Gutheinz, Chester Borden, and Yeou-Fang Wang of Caltech for NASA's Jet Propulsion Laboratory. Further information is contained in a TSP (see page 1).

This software is available for commercial licensing. Please contact Karina Edmonds of the California Institute of Technology at (626) 395-2322. Refer to NPO-44714.

TCP/IP Interface for the Satellite Orbit Analysis Program (SOAP)

The Transmission Control Protocol/Internet protocol (TCP/IP) interface for the Satellite Orbit Analysis Program (SOAP) provides the means for the software to establish real-time interfaces with other software. Such interfaces can operate between two programs, either on the same computer or on different computers joined by a network. The SOAP TCP/IP module employs a client/server interface where SOAP is the server and other applications can be clients. Real-time interfaces between software offer a number of advantages over embedding all of the common functionality within a single program. One advantage is that they allow each program to divide the computation labor between processors or computers running the separate applications. Secondly, each program can be allowed to provide its own expertise domain with other programs able to use this expertise.

For example, a telemetry acquisition system can handle the complexity of downloading data from the satellite, whereas SOAP can use such data to offer 3D displays and status information in a human-readable form. Both programs can operate efficiently, especially when they are hosted on separate machines. The SOAP TCP/IP interface supports the same rich command structure that its input file parser provides. The input is obtained and processed through the network instead of through files.

In addition, SOAP can bring additional analytical resources to bear against incoming data streams. SOAP can process these TCP/IP streams in a number of ways. It can access two simultaneous streams from different sources. This provides an added degree of flexibility in a real-time environment. The software can remain interactive while receiving data, allowing the user to configure different 3D views and data displays. For instance, a user can examine a 3D model based on orientation data streaming in from an independent source, such as the telemetry feed, or a robotic simulation such as the FORESIGHT software. Additionally, the SOAP TCP/IP interface can be configured in batch mode and reside on a server. Because SOAP can be tasked to automatically generate image and data files, it can be used to set up an automated Web site offering near real-time image and data reporting.

This software is portable and runs on four separate computer platforms: MS-Windows, Mac OS X, Linux, and Sun Solaris. There are no minimum hardware requirements other than that to run the host operating system. The host system should be capable of running OpenGL applications. SOAP performs best on the machines with good graphics hardware acceleration.

This work was done by Robert Carnright of Caltech and David Stodden and John Coggi of The Aerospace Corporation for NASA's Jet Propulsion Laboratory.

This software is available for commercial licensing. Please contact Karina Edmonds of the California Institute of Technology at (626) 395-2322. Refer to NPO-45056.

Trajectory Calculator for Finite-Radius Cutter on a Lathe

A computer program calculates the two-dimensional trajectory (radial vs. axial position) of a finite-radius-of-curvature cutting tool on a lathe so as to cut a workpiece to a piecewise-continuous, analytically defined surface of revolution. (In the original intended application, the tool is a diamond cutter, and the workpiece is made of a crystalline material and is to be formed into an optical resonator disk.) The program also calculates an optimum cutting speed as F/L, where F is a material-dependent empirical factor and L is the effective instantaneous length of the cutting edge.

The input to the program includes the analytical specification of each desired continuous piece of the surface. The output of the program corresponds to an approximate tool trajectory in the form of (1) a set of short straight-line segments connecting the precise trajectory points at user-defined axial steps and (2) the optimum cutting speed for each segment. The program includes algorithms for rounding corners, limiting the depth of cut, and making extra cutouts to prevent excessive stresses. The output of this program is read by a different program that controls stepping motors that move the cutting tool.

This program was written by Dmitry Strekalov, Anatoliy Savchenkov, and Nan Yu of Caltech for NASA's Jet Propulsion Laboratory. Further information is contained in a TSP (see page 1).

This software is available for commercial licensing. Please contact Karina Edmonds of the California Institute of Technology at (626) 395-2322. Refer to NPO-45086.

Integrated System Health Management Development Toolkit

This software toolkit is designed to model complex systems for the implementation of embedded Integrated System Health Management (ISHM) capability, which focuses on determining the condition (health) of every element in a complex system (detect anomalies, diagnose causes, and predict future anomalies), and to provide data, information, and knowledge (DIaK) to control systems for safe and effective operation.

An important functionality of ISHM is that DIaK is embedded and easily accessible. The software includes tools for distributed storage, evolution, and distribution of DIaK, and easy accessibility. For example, an intelligent sensor includes a TEDS (Transducer Electronic Data Sheet); processes for data validation and sensor health determination; communication capability to provide DIaK to other elements of the system; and to receive DIaK in order to improve its ability to validate its data and determine its own health.

The ISHM-Development Toolkit (ISHM-DTK) is an object-oriented environment that enables creation of a model of any complex system (or system-of-systems — SoS) for the ISHM embedded capability. SoS are defined as hierarchical networks of intelligent elements (sensors, components, controllers, processes, sub-systems, systems, etc.).

Integration is established by defining "Intelligent Processes" that represent models of processes that provide the means to check consistency of DIaK across the entire system. Multiple models of varying granularity and fidelity may represent a process, and they may be activated based on context. ISHM-DTK includes communications gateways to read data into the model.

ISHM-DTK allows for modular implementation of ISHM capability with almost total re-use of software. The toolkit also allows incremental implementation of ISHM capability where more and better DIaK is added as these become available or refined in the research and technology community. In order to accommodate legacy elements, such as classical sensors or components, intelligent elements may be virtually implemented in the software, or may use another software environment and/or computer in the network.

This work was done by Jorge Figueroa of Stennis Space Center and Harvey Smith and Jon Morris of Jacobs Technology.

Inquiries concerning this technology should be addressed to the Intellectual Property Manager, Stennis Space Center, (228) 688-1929. Refer to SSC-00255-1, volume and number of this NASA Tech Briefs *issue, and the page number.*


NASA
National Aeronautics and
Space Administration